Synthesis and Simple ^{18}F-Labeling of 3-Fluoro-5-(2-(2-(fluoromethyl)thiazol-4-yl)ethynyl)benzonitrile as a High Affinity Radioligand for Imaging Monkey Brain Metabotropic Glutamate Subtype-5 Receptors with Positron Emission Tomography

Fabrice G. Siméon,* Amira K. Brown, Sami S. Zoghbi, Velvet M. Patterson, Robert B. Innis, and Victor W. Pike

Molecular Imaging Branch, National Institute of Mental Health, National Institutes of Health, Building 10, Room B3 C346A, 10 Center Drive, Bethesda, Maryland 20892-1003

Received February 1, 2007

2-Fluoromethyl analogs of (3-[(2-methyl-1,3-thiazol-4yl)ethynyl]pyridine) were synthesized as potential ligands for metabotropic glutamate subtype-5 receptors (mGluR5s). One of these, namely, 3-fluoro-5-(2-(2-(fluoromethyl)thiazol-4-yl)ethynyl)benzonitrile (**3**), was found to have exceptionally high affinity (IC_{50} = 36 pM) and potency in a phosphoinositol hydrolysis assay (IC_{50} = 0.714 pM) for mGluR5. Compound **3** was labeled with fluorine-18 ($t_{1/2}$ = 109.7 min) in high radiochemical yield (87%) by treatment of its synthesized bromomethyl analog (**17**) with [^{18}F]fluoride ion and its radioligand behavior was assessed with positron emission tomography (PET). Following intravenous injection of [^{18}F]**3** into rhesus monkey, radioactivity was avidly taken up into brain with high uptake in mGluR5 receptor-rich regions such as striata. [^{18}F]**3** was stable in monkey plasma and human whole blood in vitro and in monkey and human brain homogenates. In monkey in vivo, a single polar radiometabolite of [^{18}F]**3** appeared rapidly in plasma. [^{18}F]**3** merits further evaluation as a PET radioligand for mGluR5 in human subjects.

Introduction

Glutamate is a ubiquitous excitatory neurotransmitter within the central nervous system (CNS) and acts on diverse sets of receptors, all with potential to modulate neurological function and, consequently, mental state and behavior. Glutamate receptors include NMDA, AMPA, and kainate receptors, which belong to the glutamate ionotropic receptor group. Glutamate also activates a family of G-protein-coupled receptors, the metabotropic receptors (mGluRs).[1] Based on sequence homology, functional coupling, and pharmacology,[2] mGluRs are classified as belonging to groups I, II, or III. Group I receptors are primarily localized postsynaptically and include subtype 1 (mGluR1) and subtype 5 (mGluR5), which exhibit different patterns of expression in the CNS.

Activation of mGluR5 stimulates phospholipase C, resulting in phosphoinositide hydrolysis and increase of intracellular Ca^{2+} levels.[2,3] Several potent noncompetitive antagonists for mGluR5 have been developed, including 6-methyl-2-(phenylethynyl)-pyridine[4] (MPEP; Figure 1) and 3-[(2-methyl-1,3-thiazol-4yl)-ethynyl]-pyridine[5] (MTEP; Figure 1).

Modulation of mGluR5s has potential for the treatment of schizophrenia[6] and Alzheimer's disease.[7] Further evidence supports the use of MPEP or MTEP in the treatment of anxiety,[8] depression,[9] and pain.[10] mGluR5s may also play an important role in drug-related behaviors, particularly in drug abuse,[11] drug addiction,[12] and alcohol withdrawal.[13] Hence, mGluR5 antagonists may turn out to be useful therapeutics for a variety of CNS disorders.

MPEP and MTEP have provided leads to some candidate radioligands for imaging human mGluR5 receptors with PET in vivo. Due to the small size and limited functionalization of MPEP and MTEP, labeling of their derivatives with an imaging radionuclide (e.g., carbon-11, $t_{1/2}$ = 20.4 min; fluorine-18, $t_{1/2}$ = 109.7 min; iodine-123, $t_{1/2}$ = 13.13 h) is a challenge, especially if high affinity and selectivity for mGluR5 are to be retained. Until recently, no simple derivatives of MPEP and MTEP had proven to be useful for in vivo imaging.

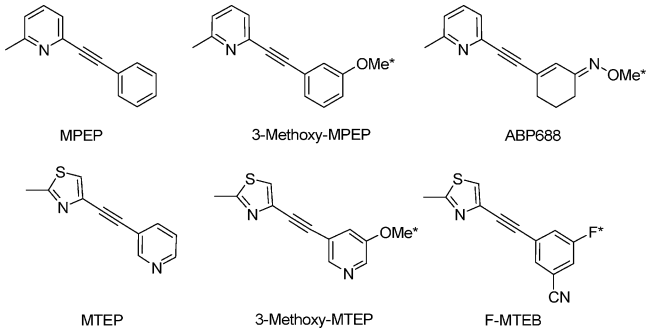

Figure 1. Structures of some mGluR5 ligands. Asterisks mark positions in which ligands have been labeled with either carbon-11 or fluorine-18.

Both ^{11}C-labeled 3-methoxy-MPEP (Figure 1)[14] and 3-methoxy-MTEP[15] (Figure 1) gave the desired rapid uptake of radioactivity into monkey and rat brain. However, this uptake was immediately followed by fast washout, suggesting little retention by high affinity receptor binding. Moreover, these radioligands showed a uniform distribution across most cerebral regions. More promising results have been obtained with [^{11}C]ABP688 (Figure 1), which was found to be a selective and effective radiotracer for imaging mGluR5 in rodents[16] and humans[17] in vivo.

Recently, researchers at Merck disclosed a selective and high affinity (K_i = 80 pM) mGluR5 ligand **(**F-MTEB, Figure 1) that, when labeled with fluorine-18, produced the first successful PET imaging of brain mGluR5s in monkey.[18] However, the radiosynthesis of this radioligand is low yielding from cyclotron-produced [^{18}F]fluoride ion (2−5%, decay-corrected) and limits the amount of radioligand that may be produced for PET studies in human subjects.

* To whom correspondence should be addressed. Tel.: 301 451 3907. Fax: 301 480 5112. E-mail: simeonf@mail.nih.gov.

10.1021/jm0701268
Published on Web 06/16/2007

Scheme 1[a]

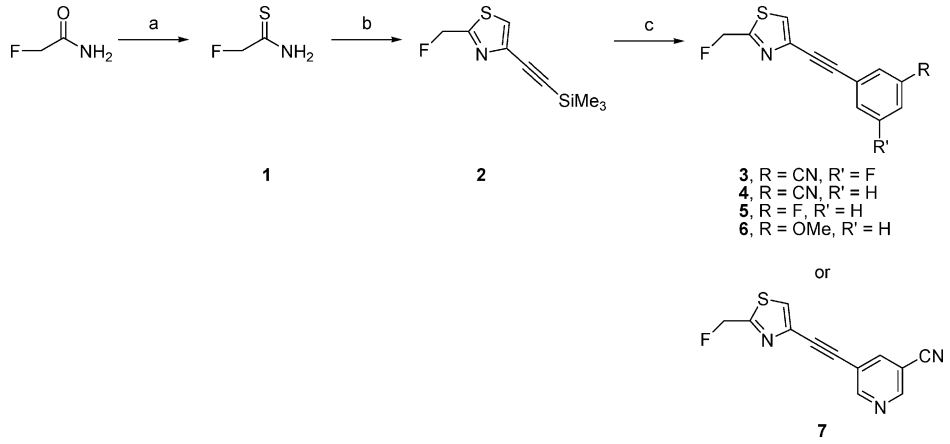

[a] Reagents, conditions, and yields: (a) Lawesson's reagent, HMPA, 80 °C, 4 h, 78%; (b) chloroacetyltrimethylsilyl−acetylene, 50 °C, 36 h, 65%; (c) ArBr, $Pd(Ph_3)_4$, CuI, DME, TBAF, 80 °C, 10−16 h, 44−70%.

Scheme 2[a]

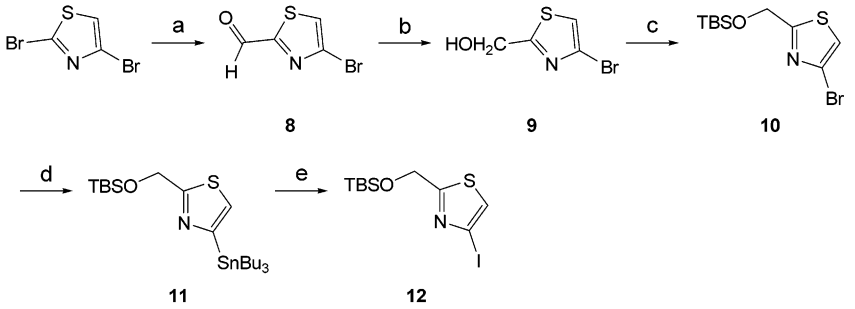

[a] Reagents, conditions, and yields: (a) BuLi, DMF, −78 °C, 30 min, ∼71%; (b) $NaBH_4$, MeOH, 25 °C, 45 min, 69%; (c) imidazole, TBSCl, CH_2Cl_2, 25 °C, 45 min, 99%; (d) BuLi, $SnBu_3Cl$, Et_2O−hexanes, −78 °C, 25 min, 71%; (e) I_2, $CHCl_3$, rt, 25 min, 96%.

We pursued a strategy for ^{18}F-labeling in a fluoromethyl group at the 2-position of a thiazole ring in mGluR5 ligands related to MTEP. By selecting this group for radiolabeling, we expected to open up a generic route to ^{18}F-labeled analogs of MTEP with almost any substitution pattern in the distal aryl ring. Based on this strategy, we now describe the synthesis of a potent mGluR5 ligand (**3**; Scheme 1) and its high-yield one-step labeling with [^{18}F]fluoride ion to give a new radioligand for imaging brain mGluR5 in vivo.

Results and Discussion

Chemistry. 2-Fluoromethylthiazole derivatives were synthesized in three-steps from commercially available materials (Scheme 1). Thiation of 2-fluoroacetamide gave 2-fluorothioacetamide (**1**), which was then cyclized by treatment with chloroacetyltrimethylsilylacetylene to give 2-(fluoromethyl)-4-(2-(trimethylsilyl)ethynyl)thiazole (**2**). The reaction, which was very slow at room temperature, reached a conversion of 89% (65% yield after purification) when heated to 50 °C for 36 h. Alkyne **2** was used as a synthon for the preparation of several new ligands (**3**−**7**) through Sonogashira[19] cross-coupling reactions.

We envisaged that the radiolabeling of ligands **3**−**7** might be achieved in each case through nucleophilic substitution in a 2-bromomethyl analog with cyclotron-produced [^{18}F]fluorine ion to give the corresponding candidate PET radioligand.

The preparation of such a bromo precursor required another synthetic route, here exemplified by the convergent synthesis of the 2-bromomethyl analog of **3**, namely, compound **17** (Schemes 2−4). The synthesis requires a 4-halo-thiazole derivative for Sonogashira coupling with a partner alkyne. Starting with 2,4-dibromo-thiazole, **10** was obtained using the reaction steps described previously for the synthesis of 2-hydroxymethylthiazole from 2-bromothiazole.[20,21] The 4-bromo group was well retained throughout this process. The bromo compound **10** could be used for Sonogashira coupling, but we decided to convert this into the more reactive iodo compound **12** through two high-yielding steps (d and e, Scheme 2).

Scheme 3[a]

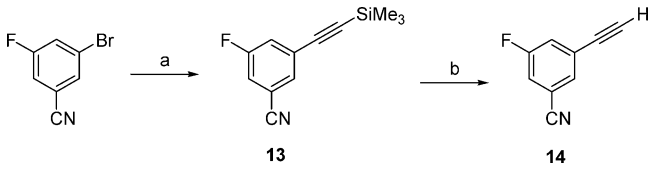

[a] Reagents, conditions, and yields: (a) TMSA, CuI, $Pd(PPh_3)_4$, DMF, rt, overnight, 94%; (b) TBAF, THF, 30 min, rt, 95%.

The coupling of 3-bromo-5-fluorobenzonitrile with trimethylsilylacetylene (TMSA) gave the silylated alkyne **13** in high yield. This was efficiently desilylated with tetrabutylammonium fluoride (TBAF) in tetrahydrofuran (THF) at room temperature to give alkyne **14** (Scheme 3).

The Sonogashira coupling of **13** or **14** with **12** gave compound **15**. As expected, the yield of **15** from **14** was much higher (90%) than from the silyl compound **13** (20%). In another experiment, we observed that the bromo derivative **10** could be coupled with **14** to give **15** in only 20% yield, so justifying the conversion of **10** into the more reactive iodo compound **12**. After treatment of **15** with TBAF, alcohol **16** was obtained in good yield. This

Scheme 4[a]

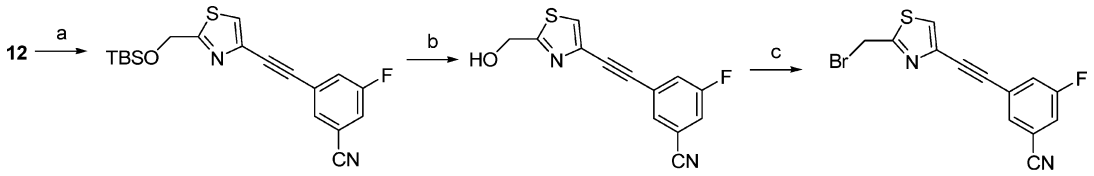

[a] Reagents, conditions, and yields: (a) **13** or **14**, CuI, $Pd(PPh_3)_4$, Et_3N, DMF, 80 °C, 10 min, 20% from **13**, 90% from **14**; (b) TBAF, THF, rt, 30 min, 82%; (c) CBr_4, PPh_3, benzene, reflux, 1 h, 51%.

Table 1. Affinities, cLogP, cLogD, and LogD Values of Ligands **3**−**7**

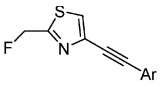

Ligand	Ar	IC_{50}[a] (nM)	cLogP[b]	cLogD[b]	LogD
3	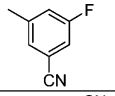	0.036 ± 0.009	3.31	3.31	2.18 ± 0.22 (n = 6)
4	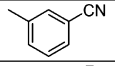	0.06 ± 0.01	2.89	2.89	
5	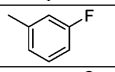	0.48 ± 0.01	3.34	3.34	
6	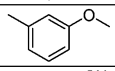	0.52 ± 0.016	3.14	3.14	
7	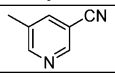	0.23 ± 0.01	1.68	1.68	

[a] All values represent the mean ± SEM of three determinations, with each determination lying within 0.3 log unit of the mean. [b] cLogP was calculated by using the Pallas 3.0 software (Compudrug, U.S.A.).

was brominated with carbon tetrabromide in the presence of triphenylphosphine to give the desired precursor **17** (Scheme 4).

Measurement and Calculation of LogD and LogP. The LogD of [^{18}F]**3** was found experimentally to be 2.18 ± 0.22 (n = 6; Table 1) and cLogD and cLogP were each computed to be 3.31. These values are within the range generally considered desirable for a prospective brain imaging agent.[22,23] cLogD values for ligands **4**−**7** were in the range 1.68−3.34. For each ligand, **3**−**7**, cLogP values were identical to cLogD values because these compounds are nonionized at physiological pH (7.4; Table 1).

In Vitro Binding Assay. All the prepared 2-fluoromethyl ligands **3**−**7** exhibited subnanomolar affinity for mGluR5s (Table 1). The direct 2-methyl analogs of ligands **3**−**6** are known and their affinities for binding to mGluR5 are reported.[18,24] Thus, the direct 2-methyl derivative of ligand **3** (F-MTEB) is reported to have a K_i value of 80 pM in a radioligand binding assay,[18] while the direct 2-methyl analogs of ligands **4**−**6** are reported to have IC_{50} values of 0.94, 23, and 49 nM, respectively, for inhibition of agonist-induced phosphoinositide hydrolysis.[24] Although these data are not strictly comparable between each other and with those of Table 1 because of differences in type of assay employed, it appears that the introduction of fluorine at the 2-methyl group is without detriment to binding affinity; that is, introduction of a fluoro substituent at the 2-methyl group allows high affinity for mGluR5 to be retained.

Introduction of a 3-nitrile group enhanced affinity for mGluR5 (cf. **3** and **5**). Reducing the lipophilicity by introducing a pyridinyl moiety, as in **7**, in place of a phenyl moiety (cf. **4**) somewhat reduced affinity.

Ligand **3** bound with exceptionally high affinity to the mGluR5 receptor (IC_{50} = 36 pM), an affinity similar to that reported for its direct 2-methyl analog, F-MTEB (K_i = 80 pM).[18] Also, **3** exhibited just slightly lower cLogP and cLogD (3.31) than F-MTEB (cLogP and cLogD = 3.32; cf. LogD = 3.2 (reported in ref 16)). In view of the similarity of properties between **3** and F-MTEB and the reported effectiveness of [^{18}F]F-MTEB as a PET radioligand,[18] we selected **3** for further study, including receptor screening, labeling with fluorine-18, and in vitro and in vivo studies.

Scheme 5[a]

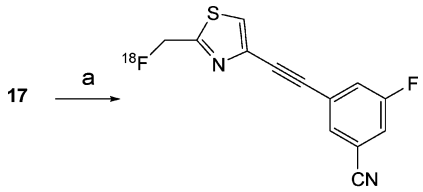

[a] Reagents, conditions, and RCY: (a) [^{18}F]fluoride ion, K_2CO_3, Kryptofix2.2.2, MeCN, 45 W in two 1-min pulses, 85 °C, 87% RCY.

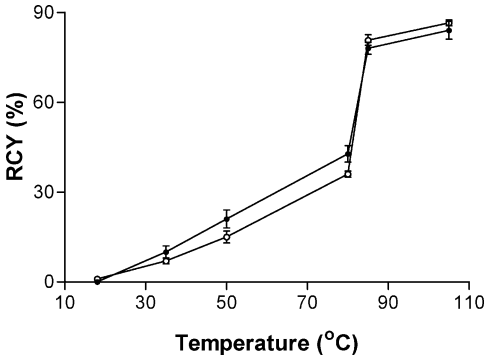

Figure 2. Variation with temperature in the decay-corrected radiochemical yields (RCYs) of [^{18}F]**3** from the radiofluoridation of **17** in acetonitrile−trace water with $KHCO_3$-18 crown-6 as base. Key: 10 min reaction, ●; 20 min reaction, ○. Points show mean of data (n = 2) and error bars show the minimum and maximum value.

Phosphoinositol Hydrolysis Assay of 3 and F-MTEB. Ligand **3** exhibited an exceptionally high potency (IC_{50} = 0.714 pM, n = 6) for inhibition of phosphoionisitol hydrolysis in this assay,[4] higher than that exhibited by F-MTEB in the same assay (IC_{50} = 9.4 pM, n = 6).

Receptor Screening of 3. Ligand **3** was found to be highly selective for binding to mGluR5 receptors over $mGluR_{1,2,4,6,\text{ and }8}$, $5\text{-}HT_{1A,1B,1D,1E,2A,2B,2C,3,5A,6,\text{ and }7}$, $\alpha_{A,1B,2A,2B,\text{ and }2C}$, $\beta_{1\text{ and }2}$, D_{1-5}, σ_1, NMDA/MK801, H_{1-4}, M_{1-5}, DOR, MOR, KOR, DAT, NET, SERT (all K_i > 10 μM).

Radiochemistry. The conversion of **17** into [^{18}F]**3** was initially investigated using Kryptofix 2.2.2-K_2CO_3 as base in acetonitrile (Scheme 5). Reaction for 30 min at 80 and 110 °C gave decay-corrected radiochemical yields (RCYs) of 48 and 77%, respectively. We next found that radiofluoridation conditions described recently in our laboratory[25] (18-crown-6-$KHCO_3$

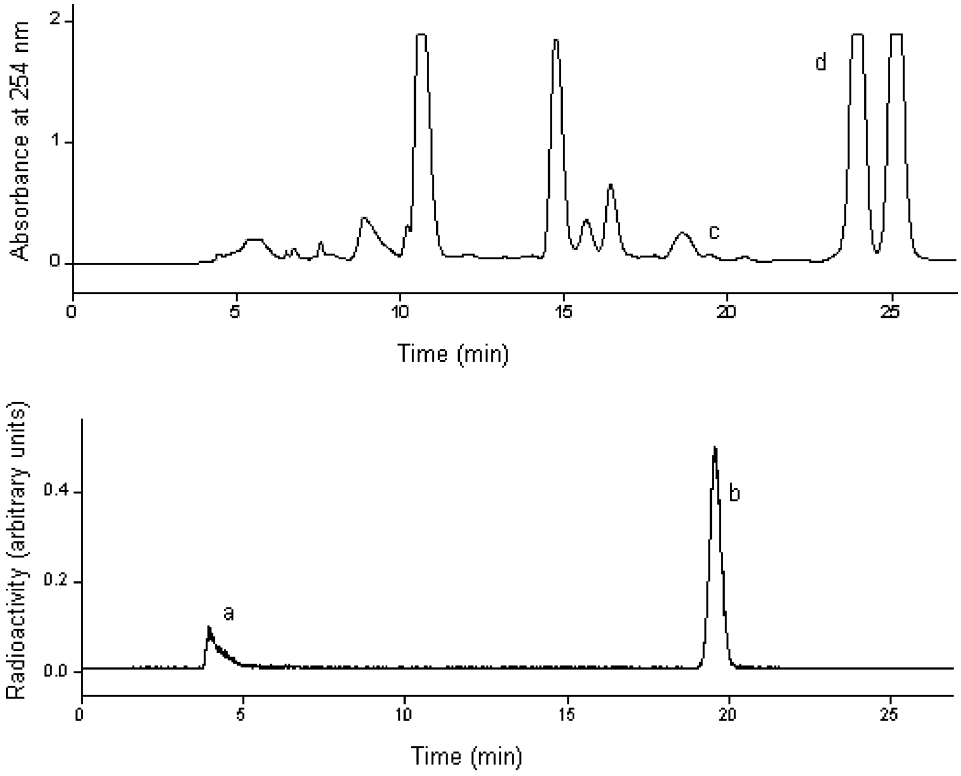

Figure 3. Chromatograms from the HPLC separation of [^{18}F]**3**, produced in a Synthia device. Key: a, [^{18}F]fluoride ion; b, [^{18}F]**3**; c, **3**; d, **17**.

in MeCN−trace H_2O) gave very high RCYs from short reaction times (10 or 20 min) at moderate temperature (80 or 85 °C). RCYs reached near maximal values after 10 min heating; they were only slightly improved with longer heating (20 min; Figure 2). Longer reaction times (>30 min) gave lower RCYs and higher temperatures (>85 °C), only slightly increased RCYs, probably due to precursor degradation in each case. No exchange of the aryl fluoro group with [^{18}F]fluoride ion was observed under these mild conditions.

For the production of [^{18}F]**3** in a formulated form ready for intravenous injection into monkey, higher starting activities of [^{18}F]fluoride ion (>100 mCi) needed to be used. Productions were initially performed within a lead-shielded automated TRACERlab FX_{F-N} apparatus. The use of anhydrous acetonitrile at 88 °C with Kryptofix 2.2.2-K_2CO_3 as base gave reproducible yields (overall isolated RCYs; 15−25%). These isolated RCYs were increased considerably (to 54%) when using microwave irradiation (45 W, 82−85 °C, 2 min) for the same radiofluoridation reaction in a lead-shielded Synthia device.[26] The incorporation of [^{18}F]fluoride ion into [^{18}F]**3** was up to 87%, decay-corrected. The radioligand was readily purified by HPLC (Figure 3) in high chemical purity (>95%), high radiochemical purity (>99%), and with specific activities up to 9 Ci/μmol at the end of synthesis (about 150 min from the end of radionuclide production).

PET Imaging in Monkey. Time−activity curves (TACs) were obtained for striata, hippocampus, occipital cortex, cerebellum, and mandible. In experiments in which [^{18}F]**3** was administered alone (baseline experiments), brain uptake of radioactivity was high, ranging between 450 and 700% SUV across regions. Hamill et al.[18] reported that, after administration of [^{18}F]F-MTEB into rhesus monkey, the uptake of radioactivity into brain was maximally about 320% SUV in striatum. (In our PET experiment with [^{18}F]F-MTEB, we found the maximal uptake of radioactivity to be similar to that of [^{18}F]**3**, i.e., 600−900% SUV across all regions.) The brain distribution of radioactivity by 180 min after administration of [^{18}F]**3** matched the expected distribution of mGluR5 receptors,[18] with regions of high receptor density (e.g., striatum; B_{max} ~63 nM in rhesus monkey caudate[18]) having high levels of radioactivity and receptor-poor cerebellum (B_{max} ~ 24 nM in rhesus monkey[18]) having a low level of radioactivity (panel A, Figure 4).

The uptake of radioactivity in mGluR5-rich regions (e.g., striata and hippocampus) and moderately rich cerebellum were reduced to about the same level when [^{18}F]**3** was administered at 15 min after a receptor saturating dose of the mGluR5-selective ligand MTEP (5 mg/kg, i.v.; panel B, Figure 4), thereby showing that there was a substantial mGluR5-specific signal in gray matter regions in the baseline experiment. Figure 5 shows horizontal PET scans acquired between 60 and 180 min after injection of [^{18}F]**3** in brain regions at the level of the striata in both a baseline and a pretreatment experiment in the same monkey. Radioactivity in the baseline experiment largely localizes to mGluR5-rich regions (e.g., striata), as shown by coregistration of brain structures with an MRI scan. In the pretreatment experiment, radioactivity is greatly diminished and uniform across the brain. One displacement study was performed in rhesus monkey, with MTEP (3 mg/kg) given at 40 min after the injection of [^{18}F]**3** (3.44 mCi). This showed a marginally quicker washout of radioactivity from mGluR5 high-density regions, including the striatum and hippocampus. A more striking effect was achieved when **3** (2 mg/kg, i.v.) was used as displacing agent at 40 min (see Supporting Information).

Under baseline conditions, radioactivity gradually accumulated in mandible, indicative of some defluorination of the radioligand to [^{18}F]fluoride ion, and reached values of about 400% SUV at 180 min (panel A, Figure 4). Because of the relatively high uptake in adjacent neocortex, we could not accurately measure skull uptake without spillover of activity from brain.

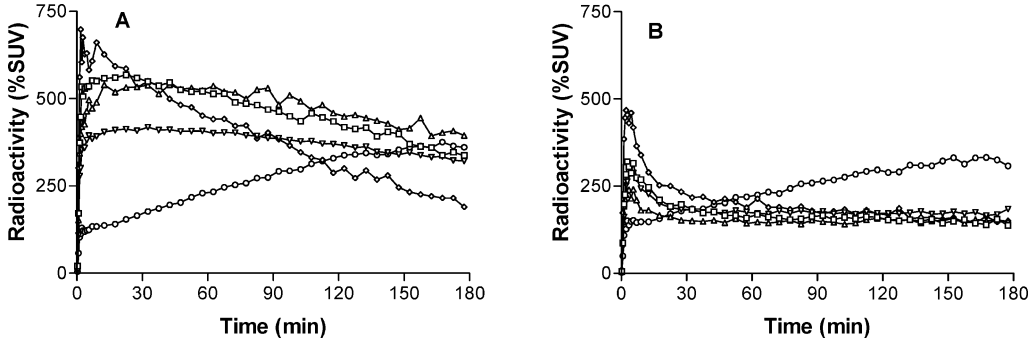

Figure 4. Time-activity curves in brain regions after (panel A) intravenous injection of [^{18}F]**3** (4.0 mCi) alone into rhesus monkey and (panel B) after intravenous injection of [^{18}F]**3** (3.8 mCi) into the same rhesus monkey at 15 min after intravenous injection of MPEP (5 mg/kg). Key: cerebellum, ◇; occipital cortex, ▽; hippocampus △; striatum, □; mandible, ○.

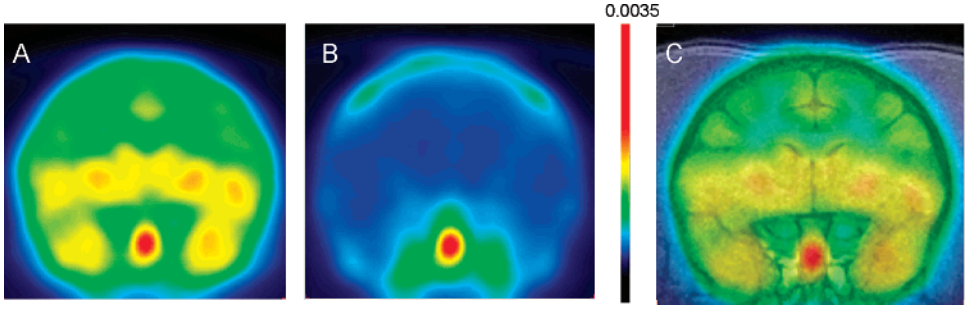

Figure 5. Horizontal PET images, obtained at the level of the striata, summed from data acquired between 60 and 180 min after injection of rhesus monkey with [^{18}F]**3** (4.0 mCi) alone (panel A) or after injection in the same monkey with [^{18}F]**3** (3.8 mCi) at 15 min later than injection of MPEP (5 mg/kg, i.v.; panel B). Panel C shows the corresponding fused magnetic resonance-PET image used to identify structures in the PET scans.

In this study, the percentage of specific (i.e., receptor-bound) radioligand in brain was not quantified with arterial sampling and compartmental modeling. As described below, [^{18}F]**3** was unstable in the whole blood of monkey and was difficult to measure with rapid sampling. Nevertheless, the brain−time activity curves allow an estimate of specific and nondisplaceable uptake, with the latter including nonspecific binding plus free radioligand in tissue water. Early time points are highly affected by blood flow and passage of the radioligand through the blood-brain barrier. During the period 60 to 120 min, when uptake is more dependent on receptor binding, uptake in hippocampus and striatum was about 500% SUV at baseline and about 200% SUV after blockade (Figure 4). Thus, about 40% of uptake in these regions appeared to be nondisplaceable and 60% specific. These estimates are prone to error because they were not corrected for any changes in the concentration of parent radioligand in plasma that may be associated with preblockade. In other words, visual inspection of the baseline and preblocked time−activity curves confirm a substantial amount of receptor-specific binding, but accurate quantitation is impossible without knowledge of arterial plasma concentrations of the parent radioligand over time.

Emergence of Radio-Metabolite in Monkey Blood In Vivo. For whole monkey blood collected from 1 to 180 min after the administration of [^{18}F]**3** into rhesus monkey, radioactivity distributed 33.9 ± 5.5% (n = 24) into cellular components. MTEP had no influence on this distribution (data not shown).

After administration of [^{18}F]**3** to monkey, radioactivity cleared quite rapidly from plasma (Figure 6). Extraction of radioactivity from plasma into HPLC analyte was generally quite efficient (79−86%), although plasma taken at certain time points (3, 5, and 10 min) gave lower extractions (65, 52, and 48%, respectively). Reverse phase radio-HPLC analysis of plasma showed that a single radio-metabolite appeared rapidly and

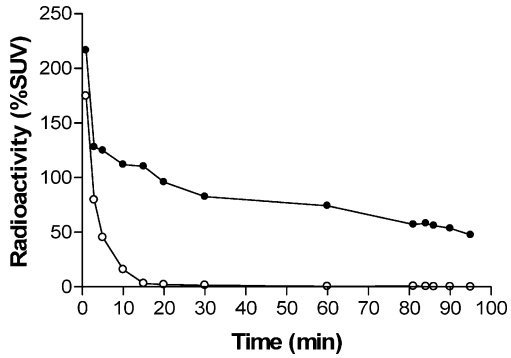

Figure 6. Clearance of total radioactivity (○) and parent radioligand radioactivity (●) from rhesus monkey plasma after administration of [^{18}F]**3**.

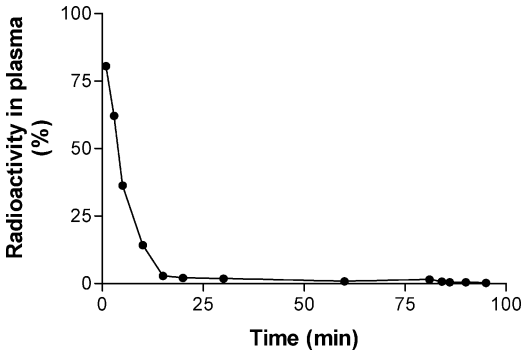

Figure 7. Time course of percentage of radioactivity in plasma represented by parent radioligand after intravenous injection of rhesus monkey with [^{18}F]**3**.

represented nearly all the radioactivity by 25 min (Figure 7). This radio-metabolite eluted near the void volume (t_R = 2.0 ± 0.04 min, n = 14) and was much more polar than parent

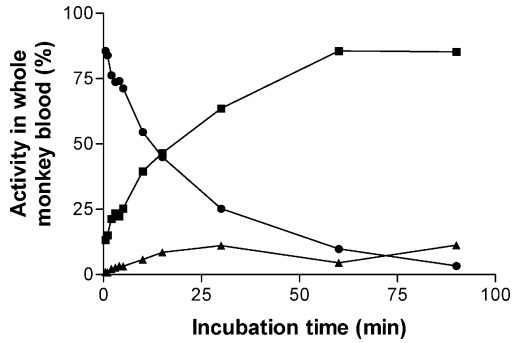

Figure 8. Time course of composition of radioactivity in whole monkey blood after addition of [^{18}F]**3**. Key: ●, [^{18}F]**3**; ■, polar radiometabolite; ▲, radioactivity not extracted into analyte.

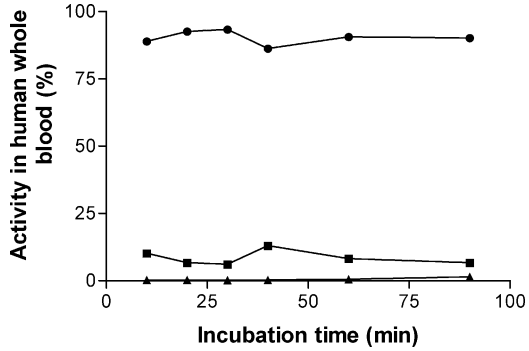

Figure 9. Time course of composition of radioactivity in whole human blood after addition of [^{18}F]**3**. Key: ●, [^{18}F]**3**; ■, polar radiometabolite; ▲, radioactivity not extracted into analyte.

radioligand (t_R = 4.8 ± 0.2 min, n = 14). In view of the observed uptake of radioactivity into mandible and the polarity of the radio-metabolite, its identity is likely to be [^{18}F]fluoride ion. The uptake of [^{18}F]fluoride ion into skull has potential to compromise accurate quantitation of receptor-radioligand interactions in closely proximal brain regions. However, the peripheral metabolism of [^{18}F]**3** in monkey does not appear to generate brain-penetrant radio-metabolites that would be troublesome for quantitation throughout the brain. It may be noted that in rhesus monkey [^{18}F]F-MTEB is not defluorinated but gives two less polar radio-metabolites in plasma (Zoghbi, S. S. et al.; unpublished results). We do not know whether these radio-metabolites may enter the brain.

Stability of [^{18}F]3 in Monkey and Human Whole Blood In Vitro. [^{18}F]**3** was found to be stable when incubated in aqueous solution for 159 min, in phosphate-buffered saline (pH = 7.4) for 71 min or in monkey plasma for 168 min. Incubation of [^{18}F]**3** with monkey whole blood over 90 min at 37 °C resulted in progressive metabolism of the radioligand predominantly to a radioactive component that was not extracted into acetonitrile and also to an acetonitrile-soluble component eluting at the void volume on reverse phase HPLC (Figure 8), consistent with possible identity (in each case) as [^{18}F]fluoride ion. This metabolism was unaffected by azide ion, which, because of its negative charge, is assumed to be unable to enter blood cells. These findings suggest that the metabolism occurs in cellular elements of monkey blood and not in plasma.

Incubation of [^{18}F]**3** with human whole blood gave strikingly different results to those of monkey whole blood. Over the time span of the experiment (90 min), the extraction of radioactivity into acetonitrile was high and this radioactivity was found to be predominantly (>98%) parent radioligand (Figure 9).

Stability of [^{18}F]3 in Monkey and Human Brain Homogenate In Vitro. [^{18}F]**3** degraded only to very low extent (1.8%) during its incubation in vitro with monkey brain homogenate at 37 °C for 90 min. The extraction of radioactivity into HPLC analytes was high (95−98%). Similarly, [^{18}F]**3** degraded only 1.4% during its incubation in vitro with human brain homogenate at 37 °C for 3 h. Extractions of radioactivity into analytes were again high (96−98%).

Conclusions

Several 2-(fluoromethyl)thiazoles were prepared as high affinity ligands for mGluR5 and as prospective PET radioligands. Introduction of a fluorine atom into the methyl group at the 2-position of the 1,3-thiazole ring was beneficial to the affinity of ligands for mGluR5 and also allowed easy labeling with [^{18}F]fluoride ion. Labeling at this position allows multiple variations in the substitution pattern of the distal aryl (phenyl or pyridinyl) ring in a search for effective PET radioligands. The new synthon 2 is exceptionally useful for preparing such ligands through Sonogashira cross-coupling reactions with substituted bromobenzenes. The new radioligand [^{18}F]**3** shows high penetration into rhesus monkey brain and a substantial percentage of brain uptake is displaceable (i.e., specifically bound to mGluR5). Quantitation of monkey brain uptake was limited because the radioligand was metabolized in whole blood of this species. We found that [^{18}F]**3** was, however, stable in human whole blood, suggesting that compartmental quantitation will be feasible in human species. In summary, [^{18}F]**3** shows promise as a new PET radioligand for quantifying mGluR5 receptors and merits evaluation in human subjects.

Experimental Section

Materials and general methods. [^{3}H]3-Methoxy-5-(pyridine-2-yl-ethynyl)-pyridine ([^{3}H]MPEPy;[27] 84 Ci/mmol) was purchased from Amersham Biosciences (Buckinghamshire, England). MPEPy was purchased from Tocris Bioscience (Ellisville, MO). 2,4-Dibromothiazole was obtained from Frontier Scientific Inc. (Logan, UT). 3-Bromo-5-fluoro-benzonitrile was obtained from Oakwood Products Inc. (West Columbia, SC). THF was freshly distilled over sodium with benzophenone before use. Methanol was dried by passage through a short column of neutral alumina. Other reagents and solvents were purchased from Aldrich Chemical Co. or Lancaster Chemical and used without further purification unless otherwise indicated. All reactions were performed under argon unless otherwise indicated.

The ^{1}H (400 MHz), ^{19}F (376.5 MHz), and ^{13}C NMR (100 MHz) spectra of all compounds were acquired on an Advance (Bruker) spectrometer using the chemical shifts of residual deuterated solvent as internal standard; chemical shifts (δ) for the proton and carbon resonance are reported in parts per million (ppm) downfield from TMS (δ = 0). Thin layer chromatography (TLC) was performed with silica gel layers (type 60 F254; EM Science), and compounds were visualized under UV light. Flash chromatography was carried out using a Horizon HPFC system (Biotage, Charlottesville, VA; column sizes: 12 × 150 mm, 25 × 150 mm, and 40 × 150 mm) with hexanes and ethyl acetate (EtOAc) as eluents. Constituent proportions in chromatographic mobile phases are expressed by volume. HPLC for determination of compound purity was performed on a Prodigy column (5 μm, 250 × 4.6 mm; Phenomenex, Torrance, CA) eluted with 10 mM ammonium formate−acetonitrile (40: 60 v/v) at 1.25 mL/min. HPLC eluates were monitored both for absorbance at 254 nm and, where appropriate, for radioactivity.

Mass spectra were acquired with a PolarisQ GC-MS instrument (Thermo Finnigan) equipped with a capillary RTX-5ms column (30 m × 0.25 mm; flow rate, 1 mL/min; carrier gas, He). High-resolution mass spectra were acquired under electron ionization conditions using a double-focusing high-resolution mass spectrometer (AUTOSPEC, Micromass Inc.) with samples introduced through a direct insertion probe. Yields are recorded for chromatographically and spectroscopically (^{1}H NMR) pure materials.

2-Fluorothioacetamide (1). Hexamethylphosphoramide (HMPA; 12 mL) was added to Lawesson's reagent[28] (4.05 g, 10 mmol) and 2-fluoroacetamide (1.54 g, 20 mmol). The reaction mixture was heated to 80 °C and stirred for 4 h, then cooled, poured into water, and extracted three times with AcOEt (40 mL). The organic phases were combined, dried over $MgSO_4$, and evaporated to dryness under vacuum. The residue was purified on a silica gel column (hexane−diethyl ether, 80:20 to 70:30) to give **1** (1.45 g, 78%) as an oil that rapidly turned into yellow crystals. ^{1}H NMR ($CDCl_3$) δ 5.12 (d, J = 48.0 Hz, 2H); ^{13}C NMR ($CDCl_3$) δ 200.7 (d, J = 12.0 Hz), 85.0 (d, J = 194 Hz); GC-MS m/z 93.01 (M^+) and 95.01 ($M + 2H^+$).

2-(Fluoromethyl)-4-(2-(trimethylsilyl)ethynyl)thiazole (2). 1-Chloro-4-(trimethylsilyl)-3-butyne-2-one (2.46 g, 14.1 mmol) was placed in *N*,*N*-dimethylformamide (DMF; 20 mL). Compound **1** (1.01 g, 10.85 mmol) was added and the mixture was heated to 50 °C for 36 h. The reaction mixture was then cooled, poured into water (50 mL), and extracted twice with AcOEt (20 mL). The organic layers were combined and dried. Solvent was then evaporated off under vacuum. The residue was purified on silica gel to give **2** (1.3 g, 65%) as a heavy oil that slowly crystallized. ^{1}H NMR ($CDCl_3$) δ 7.55 (d, J = 0.92 Hz, 1H), 5.60 (dd, J_1 = 48.0 Hz, J_2 = 0.66 Hz, 2H, CH_2), 0.26 (s, 9H); ^{13}C NMR ($CDCl_3$) δ 164.8 (d, J = 24.93 Hz), 137.9, 124.6 (d, J = 2.13 Hz), 97.8, 95.7, 81.9 (d, J = 170.0 Hz), −0.2; mp 42−44 °C; HRMS calcd for $C_9H_{13}FNSiS$ ($M^+ + H$), 214.0522; found, 214.0503.

General Method for the Sonogashira Cross-Coupling of 2 with Aryl Bromides. Compound **2** (250 mg, 1.17 mmol), the appropriate aryl bromide (1.4 mmol), CuI (15 mg, 79 μmol), Pd(PPh_3)$_4$ (45 mg, 39 μmol), and triethylamine (0.8 mL) were added to dimethylethylene glycol (DME; 8 mL). Argon was bubbled into the resulting dark solution while it was heated to 80 °C. TBAF (2 mmol; 1.0 M solution in THF, 2 mL) was added via syringe over 45 min. The resulting black reaction mixture was heated at 80 °C until TLC analysis showed no starting material present (10−16 h). The reaction mixture was cooled to room temperature, filtered through celite, and then evaporated to dryness. The resulting dark residue was dissolved in dichloromethane (25 mL) and washed with water (2 × 20 mL) and then brine (2 × 20 mL). The organic phase was dried over $MgSO_4$, evaporated under vacuum, and purified by chromatography on silica gel (hexane−AcOEt, 80:20 to 60:40).

3-Fluoro-5-(2-(2-(fluoromethyl)thiazol-4-yl)ethynyl)benzonitrile (3). Sonogashira cross-coupling was applied to 3-bromo-5-fluorobenzonitrile (280 mg; 1.4 mmol) to afford **3** (134 mg, 44%) as a white powder. ^{1}H NMR ($CDCl_3$) δ 7.69 (s, 1H), 7.64 (s, 1H), 7.48 (m, 1H), 7.36 (dd, J = 7.74 Hz, J = 1.30 Hz, 1H), 5.65 (d, 2H, J = 46.5 Hz, CH_2); ^{13}C NMR ($CDCl_3$) δ 165.3 (d, J = 25.08 Hz), 161.9 (d, J = 251.1 Hz), 136.5, 131.2 (d, J = 3.53 Hz), 125.5 (d, J = 1.94 Hz), 123.5 (d, J = 9.82 Hz), 123.2 (d, J = 23.03 Hz), 119.4 (d, J = 24.71 Hz), 116.8 (d, J = 3.11 Hz), 114.4 (d, J = 10.20 Hz), 86.1, 85.7 (d, J = 3.28 Hz), 80.6 (d, J = 170.71 Hz); mp 110−112 °C; HRMS calcd for $C_{12}H_8F_2NS$ ($M^+ + H$), 261.0298; found, 261.0306; HPLC (t_R = 7.45 min; >99.8% purity).

3-(2-(2-(Fluoromethyl)thiazol-4-yl)ethynyl)benzonitrile (4). Sonogashira cross-coupling was applied to 3-bromobenzonitrile (255 mg, 1.4 mmol) to afford **4** (162 mg; 56%) as a slightly yellow powder. ^{1}H NMR ($CDCl_3$) δ 7.77 (dd, J_1 = 7.88 Hz, J_2 = 1.16 Hz, 1H), 7.66 (s, 1H), 7.64 (dd, J_1 = 8.0 Hz, J_2 = 1.30 Hz, 1H), 7.49 (d, J = 7.84 Hz, 1H), 7.36 (dd, 1H, J = 7.0 Hz, J = 6.4 Hz), 5.65 (d, 2H, J = 46.73 Hz, CH_2); ^{13}C NMR ($CDCl_3$) δ 165.1 (d, J = 24.96 Hz), 136.9, 135.8, 135.0, 132.0, 129.4, 124.8 (d, J = 2.07 Hz), 123.9, 117.9, 113.1, 86.9, 85.0, 80.6 (d, J = 170.54 Hz); mp 82−83 °C; HRMS calcd for $C_{13}H_8FN_2S$ ($M^+ + H$), 243.0392; found, 243.0385; HPLC (t_R = 6.37 min; >99.8% purity).

2-(Fluoromethyl)-4-(2-(3-fluorophenyl)ethynyl)thiazole (5). Sonogashira cross-coupling was applied to 1-fluoro-3-bromobenzene (245 mg; 1.4 mmol) to afford **6** (193 mg, 70%) as a white powder. ^{1}H NMR ($CDCl_3$) δ 7.59 (d, J = 7.8 Hz, 1H), 7.55 (s, 1H), 7.41 (d, J = 7.1 Hz, 1H), 7.36 (m, 1H), 7.30 (dd, J = 7.74 Hz, J = 6.9 Hz, 1H), 5.58 (d, J = 47.5 Hz, 2H, CH_2); ^{13}C NMR ($CDCl_3$) δ 163.2 (d, J = 24.96 Hz), 163.2 (d, J = 255.5 Hz), 137.4, 132.4 (d, J = 3.55 Hz), 130.2 (d, J = 3.0 Hz), 127.7 (d, J = 2.05 Hz), 124.2 (d, J = 22.11 Hz), 123.9 (d, J = 9.77 Hz), 118.5 (d, J = 21.10 Hz), 114.9 (d, J = 11.5 Hz), 83.9, 81.5 (d, J = 168.00 Hz); mp 110−112 °C; HRMS calcd for $C_{12}H_8F_2NS$ ($M^+ + H$), 236.0346; found, 236.0336; HPLC (t_R = 9.15 min; >99.8% purity).

2-(Fluoromethyl)-4-(2-(3-methoxypheny)ethynyl)thiazole (6). Sonogashira cross-coupling was applied to 3-bromoanisole (262 mg; 1.4 mmol) to afford **7** (185 mg; 64%) as a beige powder. ^{1}H NMR ($CDCl_3$) δ 7.60 (s, 1H), 7.27 (m, 1H), 7.16 (ddd, d, J_1 = 1.16 Hz, d, J_2 = 1.24 Hz, d, J_3 = 7.56 Hz, 1H), 7.10 (dd, d, J_1 = 1.40 Hz, d, J_2 = 1.16 Hz, 1H), 6.92 (ddd, d, J_1 = 1.00 Hz, d, J_2 = 1.64 Hz, d, J_3 = 8.32 Hz, 1H), 5.64 (d, J = 46.77 Hz, 2H, CH_2), 3.82 (s, 3H); ^{13}C NMR ($CDCl_3$) δ 164.69 (d, J = 24.85 Hz), 159.31, 137.74, 129.50, 124.32, 123.67 (d, J = 2.16 Hz), 123.08, 116.42, 115.69, 89.44, 82.47, 80.67 (d, J = 170.3 Hz), 55.32; mp 61−62 °C; HRMS calcd for $C_{13}H_{11}FNOS$ ($M^+ + H$), 248.0545; found, 248.0555; HPLC (t_R = 8.48 min; >99.8% purity).

5-(2-(2-(Fluoromethyl)thiazol-4-yl)ethynyl)pyridine-3-carbonitrile (7). Sonogashira cross-coupling was applied to 3-bromo-5-cyanopyridine (256 mg, 1.4 mmol) to afford **5** (128 mg, 45%) as a white powder. ^{1}H NMR ($CDCl_3$) δ 8.96 (s, 1H), 8.84 (s, 1H), 8.09 (t, J = 1.90 Hz, 1H), 7.37 (s, 1H), 5.66 (d, 2H, J = 46.65 Hz, CH_2); ^{13}C NMR ($CDCl_3$) δ 165.50 (d, J = 25.05 Hz), 155.16, 151.13, 141.27, 136.25, 125.81 (d, J = 2.05 Hz), 120.23, 115.73, 110.02, 88.48, 83.64, 80.59 (d, J = 170.74 Hz); mp 142−144 °C; HRMS calcd for $C_{12}H_7FN_3S$ ($M^+ + H$), 244.0345; found, 244.0340; HPLC (t_R = 5.10 min; >99.8% purity).

4-Bromothiazole-2-carbaldehyde (8). To a solution of 2,4-dibromothiazole (1 g, 4.12 mmol) in anhydrous ether (40 mL, 0.1 M) at −78 °C was added *n*-BuLi (1.6 M in hexanes, 4.94 mmol, 3.08 mL). The resulting solution was stirred at the same temperature for 45 min. DMF (0.64 mL, 8.24 mmol) was then added at −78 °C. The reaction mixture was stirred at −78 °C for 30 min and then slowly warmed to 25 °C over 2 h. Hexane (20 mL) was added, and the resulting mixture was passed through a short silica gel cake eluted with 30% EtOAc in hexanes. The solvents were evaporated off to give the crude aldehyde **8** (558 mg, 71%), which was used directly in the next step.

(4-Bromothiazol-2-yl)methanol (9). To a solution of crude **8** (558 mg, 2.92 mmol) in methanol (2.0 mL) at 25 °C was added sodium borohydride (210 mg, 5.55 mmol). The resulting mixture was stirred at the same temperature for 45 min. EtOAc−hexane (1:1 v/v; 50 mL) was added, and the mixture was passed through a short silica gel cake eluted with EtOAc. The solvents were then evaporated off and the crude product was purified by flash column chromatography (silica gel, 20 → 50% EtOAc in hexanes) to furnish **9** (385 mg, 69%). ^{1}H NMR ($CDCl_3$) δ 7.20 (s, 1H), 4.93 (s, 2H); ^{13}C NMR ($CDCl_3$) δ 173.0, 124.4, 117.0, 61.8.

2-(*tert*-Butyldimethylsilyloxymethyl)-4-bromothiazole (10). To a solution of **9** (200 mg, 1.03 mmol) in CH_2Cl_2 (3.5 mL, 0.3 M) was added imidazole (210 mg, 2.06 mmol) followed by *tert*-butyldimethylchlorosilane (202 mg, 1.34 mmol) at 25 °C. The reaction mixture was kept at 25 °C for 45 min, quenched with MeOH (0.5 mL), and then passed through silica gel eluted with CH_2Cl_2. Evaporation of solvents gave the desired silyl ether **10** (315 mg, 99%). ^{1}H NMR ($CDCl_3$) δ 7.16 (s, 1H), 4.93 (s, 2H), 0.94 (s, 9H), 0.12 (s, 6H); ^{13}C NMR ($CDCl_3$) δ 174.5, 124.2, 116.4, 62.9, 25.7, 18.2, −5.5.

2-(*tert*-Butyldimethylsilyloxymethyl)-4-*tri*-*n*-butylstannylthiazole (11). To a solution of **10** (200 mg, 0.65 mmol, 0.07 M) in ether (10.0 mL) at −78 °C was added *n*-BuLi (1.6 M in hexanes, 0.78 mmol, 0.5 mL). The resulting mixture was stirred at −78 °C for 25 min, and then tri-*n*-butyltin chloride (230 μL, 0.78 mmol) was added. The solution was stirred at −78 °C for 25 min and then slowly warmed to 25 °C over 90 min. Then the reaction mixture was diluted with hexane (2.0 mL) and passed through silica gel eluted with 20% EtOAc in hexanes. Flash column chromatography (silica gel; pretreated with Et_3N, 5% ether in hexanes) furnished **11** (240 mg, 71%). R_f = 0.36 (silica gel, 5% EtOAc in hexanes); ^{1}H NMR (C_6D_6) δ 7.08 (s, 1H), 4.98 (s, 2H), 1.75−1.57 (m, 6H), 1.44−1.31 (m, 6H), 1.26−1.09 (m, 6H), 0.94 (s, 9H),

0.91 (t, J = 7.0 Hz, 9H), − 0.02 (s, 6H); ^{13}C NMR ($CDCl_3$) δ 173.2, 159.1, 125.3, 63.5, 29.0, 27.3, 25.8, 18.3, 13.7, 10.1, −5.4.

2-(*tert*-Butyldimethylsilyloxymethyl)-4-iodothiazole (12). A solution of iodine (51 mg, 0.2 mmol) in anhydrous chloroform (2.5 mL) was added to a solution of **11** (100 mg, 0.19 mmol) in chloroform (1.0 mL) over 10 min. The mixture was stirred at room temperature for 25 min, and the resultant dark solution was washed with a solution of sodium hydrogen carbonate (2 mL) followed with a solution of sodium hydrogen sulfite (3 mL). The organic phase was dried over magnesium sulfate and evaporated to dryness to give **12** as a viscous oil (230 mg, 96%). ^{1}H NMR ($CDCl_3$) δ 7.38 (s, 1H), 4.97 (s, 2H), 0.94 (s, 9H), 0.13 (s, 6H); ^{13}C NMR ($CDCl_3$) δ 175.7, 122.3, 93.1, 62.9, 25.7, 18.3, −5.4; HRMS calcd for $C_{10}H_{19}INOSSi$ (M^+ + H), 356.0001; found, 355.9998.

3-Fluoro-5-(2-(trimethylsilyl)ethynyl)benzonitrile) (13). 3-Bromo-5-fluorobenzonitrile (0.58 g, 2.9 mmol) and 3-(trimethylsilyl)-acetylene (0.453 g, 4.61 mmol) were placed in a double-necked flask (25 mL) loaded with dichlorobis(triphenylphosphine) palladium (100 mg, 0.15 mmol) and CuI (28 mg; 0.15 mmol) under argon. Anhydrous DMF (7 mL) and triethylamine (1.6 mL) were added, and the solution was stirred at room temperature overnight. The dark solution was filtered through celite, evaporated to dryness under vacuum, and then chromatographed on silica gel (hexane−AcOEt, 95:5 to 80:20) to give **13** (0.59 g, 94%) as a viscous yellow oil. ^{1}H NMR ($CDCl_3$) δ 7.54 (t, J = 1.30 Hz, 1H), 7.39 and 7.37 (2 dd, 1H, J_1 = 8.88 Hz, J_2 = 2.52 Hz), 7.31 and 7.29 (2 dd, 1H, J_1 = 7.86 Hz, J_2 = 2.52 Hz), 0.26 (s, 9H); ^{19}F NMR ($CDCl_3$) δ −109.49 (s); ^{13}C NMR ($CDCl_3$) δ 162.16 (d, J = 251.5 Hz), 131.86 (d, J = 4.02 Hz), 127.02 (d, J = 10.06 Hz), 123.78 (d, J = 23.14 Hz), 119.35 (d, J = 6.16 Hz), 117.25 (d, J = 3.0 Hz), 114.40 (d, J = 10.06 Hz), 101.28 (d, J = 3.02 Hz), 99.40, 0.28; HRMS calcd for $C_{12}H_{13}FNSi$ (M^+ + H), 218.0801; found, 218.0814.

3-Ethynyl-5-fluorobenzonitrile (14). Compound **13** (0.23 g, 1.15 mmol) was dissolved in anhydrous THF (12 mL) under argon within a double-necked flask (25 mL). TBAF solution (1.0 M in THF, 1.72 mL, 1.72 mmol) was added slowly to give a deep dark solution. TLC (hexane−ethyl acetate, 80:20) showed no trace of reagent at the end of addition. The reaction mixture was stirred for 30 min. Hexane (15 mL) was then added, and the solution was filtered over a short cake of silica gel. Evaporation of solvent gave 158 mg (95%) of fine volatile crystals that were used without further purification. ^{1}H NMR ($CDCl_3$) δ 7.57 (s, 1H), 7.42 (d, 1H, J_1 = 8.00 Hz), 7.42 (d, 1H, J_1 = 8.00 Hz), 3.26 (s, 1H, CH); ^{19}F NMR ($CDCl_3$) δ −109.08; ^{13}C NMR ($CDCl_3$) δ 157.78 (d, J = 251.52 Hz), 131.69 (d, J = 3.02 Hz), 125.83 (d, J = 10.06 Hz), 123.75 (d, J = 25.15 Hz), 119.53 (d, J = 25.15 Hz), 116.75, 114.00 (d, J = 10.06 Hz), 81.06, 80.06; mp 56−57 °C; HRMS calcd for C_9H_4FN (M^+ + H), 146.0406; found, 146.0409.

3-Fluoro-5-(2-(*tert*-butyldimethylsilyloxymethyl)thiazol-4-yl)-ethynyl)benzo-nitrile (15). Compounds **12** (136 mg, 0.38 mmol) and **14** (65 mg, 0.45 mmol) were added to DMF (5 mL) containing CuI (7.5 mg, 39 μmol), $Pd(PPh_3)_4$ (45 mg, 39 μmol), and triethylamine (0.44 mL, 3.12 mmol). Argon was bubbled into the solution while it was warmed to 80 °C, and the bubbling was maintained for a further 10 min at 80 °C. TLC analysis showed no starting material present in solution after 3 h. The reaction mixture was cooled to room temperature and concentrated in vacuo. The crude residue was filtered through a short cake of silica gel eluted with hexane−AcOEt (80:20), and the obtained solution was evaporated under vacuum. Chromatography on silica gel (hexane−AcOEt, 90:20 to 80:20) gave **15** (128 mg, 90%) as a yellow oil. ^{1}H NMR ($CDCl_3$) δ 7.62 (m, 1H), 7.57 (s, 1H), 7.47 (m, 1H), 7.35 (dd, J_1= 7.84 Hz, J_2= 1.36 Hz, 1H), 4.97 (s, 2H), 0.95 (s, 9H), 0.14 (s, 6H); ^{13}C NMR ($CDCl_3$) δ 174.1, 161.9 (d, J = 251.50 Hz), 135.8, 131.2 (d, J = 3.37 Hz), 126.3 (d, J = 10.06 Hz), 124.3, 123.2 (d, J = 22.8 Hz), 119.1 (d, J = 24.82 Hz), 116.8 (d, J = 3.48 Hz), 114.3 (d, J = 10.24 Hz), 86.9, 85.1 (d, J = 3.40 Hz), 63.05, 25.7, 18.24, −5.45; HRMS calcd for C_9H_4FN (M^+ + H), 373.1206; found, 373.1208.

3-Fluoro-5-(2-(2-(hydroxymethyl)thiazol-4-yl)ethynyl)benzonitrile (16). To a stirred solution of **15** (180 mg, 0.48 mmol) in anhydrous THF (5 mL) was added a solution (1 M) of TBAF (0.58 mmol) in THF (0.58 mL). The reaction mixture was maintained for 30 min at room temperature and then filtered through a short cake of silica gel eluted with AcOEt. Evaporation of solvents gave the desired alcohol **16** (150 mg). Chromatography on silica gel (CH_2Cl_2−MeOH, 94:6) gave **17** (102 mg, 82%) as a white powder. ^{1}H NMR ($CDCl_3$) δ 7.62 (s, 1H), 7.60 (s, 1H), 7.45 (m, 1H), 7.35 (d, J = 6.84 Hz, 1H), 4.98 (s, 2H); ^{13}C NMR ($CDCl_3$) δ 171.8, 161.9 (d, J = 251.39 Hz), 136.0, 131.2 (d, J = 3.50 Hz), 126.1 (d, J = 9.85 Hz), 124.6, 124.0 (d, J = 22.8 Hz), 119.3 (d, J = 24.73 Hz), 116.8 (d, J = 3.48 Hz), 114.3 (d, J = 18.18 Hz), 86.5, 85.5, 62.2; mp 127−129 °C; HRMS calcd for C_9H_4FN (M^+ + H),-259.0341; found, 259.0345.

3-(2-(2-(Bromomethyl)thiazol-4-yl)ethynyl)-5-fluorobenzonitrile (17). The alcohol **16** (30 mg, 0.116 mmol) was dissolved in benzene (1.1 mL) containing carbon tetrabromide (0.76 g, 2.30 mmol). Triphenylphosphine (0.55 mg, 0.19 mmol) was added, and the solution was heated to reflux for 1 h after which no starting material was observed in TLC. The reaction mixture was cooled to room temperature and filtered through celite. Solvent was evaporated off and chromatography on silica gel (hexane−AcOEt, 80:20) gave **17** (19 mg, 51%) as a white powder. ^{1}H NMR ($CDCl_3$) δ 7.66 (s, 1H), 7.63 (t, J = 1.24 Hz, 1H), 7.48 (ddd, J = 8.72 Hz, J = 1.34 Hz, J = 1.44 Hz, 1H), 7.37 (ddd, J = 0.80 Hz, J = 1.36 Hz, J = 1.40 Hz, 1H), 4.74 (s, 2H); ^{13}C NMR ($CDCl_3$) δ 166.3, 161.9 (d, J = 251.52 Hz), 136.3, 131.2 (d, J = 3.0 Hz), 126.2, 125.9 (d, J = 10.2 Hz), 123.2 (d, J = 23.14 Hz), 119.4 (25.0), 116.8 (d, J = 3.2 Hz), 114.3 (d, J = 10.2 Hz), 100.0, 86.2, 85.6 (d, J = 3.02 Hz); mp 102−104 °C; HRMS calcd for $C_{13}H_6BrFN_2S$ (M^+ + H), 320.9497; found, 320.9494; HPLC (t_R = 10.05 min; >99.8% purity).

Measurement of LogD and Calculation of cLogD and cLogP. The value for the partition coefficient of [^{18}F]**3** between *n*-octanol and sodium phosphate buffer (0.15 M, pH 7.4) was determined according to the general method of Zoghbi et al.[29] cLogD and cLogP values for mGluR5 ligands were calculated with Pallas 3.0 software (Compudrug; S. San Francisco, CA).

Radionuclide Production. No-carrier-added (NCA) [^{18}F]fluoride ion was produced with the ^{18}O(p,n)^{18}F reaction, by irradiating ^{18}O-enriched water (95 atom %; 1.8 mL) with a beam of protons (14.1 MeV; 20−25 μA) from a PETtrace cyclotron (GE). Generally, this method produces [^{18}F]fluoride ion with a specific radioactivity exceeding 10 Ci/μmol.

Preparation of [^{18}F]3—Experimental Labeling with Low Radioactivity. A glass V-vial (1 mL volume) was loaded with 100 μL of a pre-prepared solution of $KHCO_3$ (0.23 g) and 18-crown-6 (0.62 g) in acetonitrile−water (15:1 v/v; 10 mL). NCA [^{18}F]fluoride ion (<10 mCi) in [^{18}O]water (50−200 μL) was added to the vial and the solvent was evaporated off with heating at 110 °C under reduced pressure (controlled with a bleed of nitrogen). The reaction mixture was further dried azeotropically during three cycles of addition−evaporation of acetonitrile (0.5 mL each cycle). A solution of the precursor **17** (1.2 to 1.5 mg) in acetonitrile (0.5 mL), containing water (1 μL, 56 μmol) was added to the dry residue, and the reaction vessel was heated for a set time (10 or 20 min) and temperature (in the range 20−110 °C). The reaction mixture was cooled for 5 min and then analyzed by radio-TLC (hexane−EtOAc, 80:20; R_f [^{18}F]**3** = 0.52) or radio-HPLC.

Automated Production of [^{18}F]3 for Intravenous Injection into Monkey. A commercial automated apparatus, namely, the TRACERlab FX_{F-N} (GE Medical Systems), was used initially. This apparatus is designed for performing single-step reactions with cyclotron-produced [^{18}F]fluoride ion and for purification and formulation of the labeled product. In this apparatus, aqueous [^{18}F]-fluoride ion was dried by cycles of addition and evaporation of acetonitrile and complexed with K^+-Kryptofix 2.2.2. This complex was reacted with precursor **17** (0.8−1.2 mg) at 88 °C for 20 min. The radioactive product was purified by injection (5 mL sample loop) into a semipreparative column (Luna C18, 10 μm, 10 × 250 mm; Phenomenex) eluted at 6.5 mL/min with a mixture of 10 mM ammonium formate (A) and MeCN (B) according to the program

25% B for 3 min, increasing to 50% B over 7 min and held at 50% B for 20 min. The fraction containing [^{18}F]**3** (t_R = 22.2 min) was collected in water (100 mL). The aqueous solution was passed through a C-18 Sep-pak, and the trapped radioactive product eluted with ethanol (1 mL) into a sterile flask loaded with saline (9 mL).

The radiochemical purity and specific radioactivity of the product were calculated by injecting a sample of the radioactive solution (0.2−0.5 mCi) into a reverse phase analytical column (Luna C18, 4.6 × 250 mm, 5 μm; Phenomenex) eluted with MeCN−10 mM ammonium formate (60:40) at 2 mL/min ([^{18}F]**3**, t_R = 6.2 min). The absorbance response was calibrated with respect to the mass of **3**.

Automated production of [^{18}F]**3** was subsequently performed in a Synthia apparatus[26] adapted to use microwave irradiation for the labeling reaction.[30] A microwave reactor (model 521; Resonance Instruments Inc., Skokie, IL) was securely mounted on a Synthia MKII Lab System. The time and power control were located outside a lead-shielded hot-cell and linked to the cavity through an RF coaxial cable. The reaction V-vial (1 mL, Alltech) was equipped with a screw-on cap and septum (Tuf-Bond Teflon/silicone; Pierce), pierced with a vent needle that was connected to a glass vial (20 mL) to collect the solvents, and also a charcoal trap to retain any break-through of volatile radioactive species. Liquid handling was achieved with a Gilson Aspec auto-injector/dispenser, which forms part of the Synthia apparatus. Other operations of the radiosynthesis and purification procedures were controlled by a visual chemistry-based recipe. Heating time and power input were controlled independently. Cyclotron-produced [^{18}F]fluoride ion in ^{18}O-enriched water (350−500 μL) was dried in the V-vial containing Kryptofix 2.2.2 (5 mg) and K_2CO_3 (0.5 mg) in acetonitrile−water (9:1 v/v, 100 μL). Microwave heating (90 W in 3 pulses of 2 min) was applied under N_2 gas flow (200 mL/min) to speed up the removal of the azeotropic water−acetonitrile mixture. The heating cycle was repeated twice, and each time fresh acetonitrile (500 μL) was added. Precursor **17** (∼0.75−1.0 mg) in acetonitrile (100 μL) was introduced into the V-vial and heated at 82−85 °C (45 W in two pulses of 1 min). The reaction mixture was diluted with mobile phase (0.75 mL) and injected onto Luna C18 (5 μm, 250 × 10 mm, Phenomenex) eluted at 2.5 mL/min with a mixture of A (25 mM ammonium formate) and B (acetonitrile−25 mM ammonium formate, 75:25) according to the following program: 68% B for 2 min, then 76% B over 4 min, and finally 87% B over 30 min ([^{18}F]-**3**, t_R = 19.6 min).

In Vitro Receptor Binding Assay. The affinity of test compounds was determined by displacement of [^{3}H]MPEPy binding to rat brain membranes. Thus, whole rat brain, minus cerebellum and brainstem, was homogenized (1:10 w/v) in ice-cold assay buffer (50 mM Tris-HCl−1.1% saline buffer, pH 7.5). The homogenate was centrifuged at 39 800 *g* for 10 min at 4 °C, and the resulting pellet was resuspended in buffer (6.25 mg original wet weight per mL) and stored at −70 °C until analysis.[27] Immediately before analysis, membranes were resuspended in assay buffer (0.9% NaCl containing 50 mM Tris-HCl) to give a final assay concentration of 5 mg/800 μL. Each competing ligand (10 mM in EtOH) was added in a volume of 100 μL to give a final concentration in the range of 0.01 nM to 1 mM along with 100 μL of [^{3}H]MPEPy. The incubation was initiated by adding membranes (800 μL) to constitute a total assay volume of 1 mL and was allowed to proceed for 1 h at 22 °C. The assay was terminated by rapid filtration over Whatman GF/B filters that had been presoaked in poly(ethyleneimine) (0.5%) and then three washes with ice-cold saline (0.9% NaCl; 3 mL). Radioactivity was determined by liquid scintillation counting.

Phosphoionisitol Hydrolysis Assay. Ligands **3** and F-MTEB were tested in a CHO cell-based assay by the National Institute of Mental Health Psychoactive Drug Screening Program for their potency to inhibit phosphoionistol hydrolysis.[4]

Receptor Screening of 3. Ligand **3** was screened for binding to a wide range of receptors and transporters by the National Institute of Mental Health Psychoactive Drug Screening Program. Detailed protocols are available online for all binding assays at the NIMH−PDSP web site (http://pdsp.med.unc.edu)

Animal Care and Use. Experiments in four rhesus monkeys (*Macacca mulatto*) were conducted according to the *Guide for the Care and Use for Laboratory Animals.*[31] Rhesus monkeys (∼10 kg) were initially anesthetized with ketamine (10 mg/kg, i.m.) and then induced with propofol (5 mg/kg, i.v.), intubated, and respired with medical grade air. During the PET scanning sessions, anesthesia was maintained by continuous administration of isoflurane at 1.0−4.0% in oxygen via the endotracheal tube. Body temperature was maintained between 37 and 37.5 °C. Electrocardiograph, heart, and respiration rates were also monitored throughout the experiment.

Positron Emission Tomography. PET scans were performed in a high-resolution research tomograph (HRRT, Siemens/CPS, Knoxville, TN). Transmission scans were performed with a ^{137}Cs point source following injection of 2 to 5 mCi of the PET radioligand. Images were reconstructed with attenuation and scatter correction using a list mode OSEM algorithm,[32] resulting in an image resolution of 2.5 mm fwhm.

Tomographic images were analyzed with PMOD 2.75 (PMOD Technologies Ltd, Adliswil, Switzerland). For each scan, a static PET image was obtained by summing the dynamic frames acquired during the acquisition.

In a baseline experiment, [^{18}F]**3** (3.99 mCi; specific radioactivity, 1.93 Ci/μmol) was injected intravenously into the monkey (14.7 kg) as a bolus in physiological saline (5 mL) containing ethanol (10%). For a pretreatment experiment on a separate day, MTEP (2−5 mg/kg) in physiological saline containing ethanol (10%) was injected intravenously into the same monkey at 15 min before injection of [^{18}F]**3** (3.82 mCi; specific radioactivity, 2.02 Ci/μmol).

Regions of interest were drawn on the coregistered images in striatum (caudate and putamen), thalamus, hippocampus, occipital cortex, cerebellum, and bone (mandible). These regions were transferred onto the dynamic scans to obtain the corresponding time−activity curves. Radioactivity was expressed as standardized uptake value (SUV), which normalizes for injected activity and body weight.

$$\%\mathrm{SUV} = \%\ \text{injected activity/cm}^3\ \text{brain} \times \text{body weight (g)}$$

MRI and Image Fusion. All monkeys had T1-weighted magnetic resonance imaging (TR/TE/x = 24 ms/3 ms/300), acquired on a 1.5-T GE Horizon Instrument (General Electric Medical Systems, Waukesha, WI). PET and NMR images were coregistered with SPM2 (Wellcome Department of Cognitive Neurology, London, U.K.).

Emergence of Radio-Metabolite in Monkey Blood In Vivo. Heparinized blood samples (1 mL) were drawn at 1 min intervals for 5 min and then at 10, 25, 40, 60, 90, 120, and 180 min after injection of [^{18}F]**3** (2.2. mCi) into an anesthetized monkey. They were placed immediately on ice to retard ex vivo metabolism. Measured aliquots (by pipetting; about 1 mL) of blood were then centrifuged at 1800 *g* for 1.5 min and plasma separated. The cellular and the plasma fractions were then counted in a γ-counter. The distribution of radioactivity was calculated for each sample. The total radioactivity in the plasma and the cells represented the amount in whole blood.

Stability of [^{18}F]3 in Monkey and Human Whole Blood and Plasma In Vitro. In these experiments, the initial radiochemical purity of [^{18}F]**3** and subsequent measures of stability were determined by reverse phase chromatography on a Novapak C-18 column (100 × 8 mm; Waters Corp., Milford, MA) using a Radial−Pak compression module RCM-11 with a sentry precolumn and a mobile phase of MeOH−H_2O−Et_3N (70:30:0.1) at a flow rate of 2.0 mL/min.

To test for the stability of [^{18}F]**3** in monkey whole blood, anticoagulated (EDTA) blood (8 mL) was drawn from an anesthetized monkey. [^{18}F]**3** (15 μCi) was added to whole blood (1.5 mL), which was then sampled (50 μL) at 0.5, 1, 2, 3, 4, 5, 10, 15, 30, 60, and 90 min. Each sample was added immediately to acetonitrile

(300 μL) that had been spiked with **3**. The mixture was then agitated, diluted with water (50 μL), and mixed. The mixture was counted for radioactivity in a γ-counter and centrifuged at 9400 *g* for 1 min. The clear supernatant liquid was analyzed with HPLC and the precipitate counted for radioactivity in a γ-counter.

The effect of sodium azide on stability of [^{18}F]**3** in whole monkey blood was also assessed. Thus, whole blood (1 mL) was mixed well with a solution (20 μL) of sodium azide (6 mg). [^{18}F]**3** was added and the solution incubated at room temperature for 190 min before centrifugation at 1800 *g* for 4 min. The supernatant plasma was treated with acetonitrile and analyzed with HPLC. The stability of [^{18}F]**3** in monkey plasma was assessed as follows. Whole monkey blood (2.0 mL) was centrifuged at 1800 *g* for 5 min. Supernatant plasma (1.0 mL) was added to [^{18}F]**3** (5 μCi) and the solution incubated at RT for 168 min. A sample was then analyzed by HPLC. To test the stability of [^{18}F]**3** in whole human blood, [^{18}F]**3** (2 μCi) was added to human whole blood (2.0 mL), incubated at 23 °C, and sampled (50 μL) at 10, 15, 20, 30, 40, 60, and 90 min. Each sample was placed in acetonitrile (50 μL) that had been spiked with **3** and mixed well. Then potassium fluoride solution (0.5 M; 50 mL) was added to each sample before mixing again, counting for radioactivity in a γ-counter, and centrifugation at 10 000 *g* for 1 min. Each supernatant liquid was injected onto HPLC for analysis.

The stability of [^{18}F]**3** in aqueous solution was also checked. Thus, solutions of [^{18}F]**3** in water alone and in saline (0.9%) containing phosphoric acid (0.15 mM) were prepared and sampled at set times (34, 48, and 159 min for water solution and 54 and 71 min for salt solution) for immediate HPLC analysis.

Stability of [^{18}F]3 in Monkey and Human Brain Homogenates In Vitro. Monkey brain tissue (3.34 g), previously stored for 1 year at −70 °C, was thawed slowly at room temperature and then homogenized with [^{18}F]**3** (∼100 μCi). The tissue suspension was ice-cooled between each pass of homogenization. Brain homogenate was sampled after incubation at 37 °C in an oscillating water bath at 5, 10, 15, 30, 60, and 90 min.

Human brain tissue (1.76 g), previously stored for a few weeks at −70 °C, was thawed slowly at room temperature and then homogenized with ice-cold saline (3 mL). The tissue suspension was ice cooled between each pass of homogenization. [^{18}F]**3** (∼50 μCi) in ethanol−water (1:1 v/v; 450 μL) was slowly mixed into to the cold homogenate. This mixture was incubated at 37 °C in an oscillating water bath and sampled (50 μL) after 5, 10, 15, 30, 45, 60, 90, 120, and 180 min.

Samples from incubations of [^{18}F]**3** with monkey or human brain homogenate were added to acetonitrile (700 μL), which had been spiked with **3** and mixed well. Then potassium fluoride solution (0.5 M; 50 μL) was added, and the solution was mixed well again. Each sample was counted in a γ-counter and centrifuged at 10 000 *g* for 1 min. The supernatant liquids were analyzed with HPLC. The precipitates were counted in a γ-counter to enable calculation of the recovery of radioactivity into acetonitrile.

Acknowledgment. This research was supported by the Intramural Research Program of the National Institutes of Health (NIMH). We thank the NIH PET Department for fluorine-18 production and successful completion of the scanning studies, PMOD Technologies for providing the image analysis software, and the NIMH Psychoactive Screening Program (PDSP) for performing assays. The PDSP is directed by Bryan L. Roth, Ph.D., with project officer Jamie Driscol (NIMH) at the University of North Carolina at Chapel Hill (Contract No. NO1MH32004).

Supporting Information Available: HPLC chromatograms verifying the purities of target compounds **3**−**7** and precursor **17** and data from a PET displacement experiment in monkey with [^{18}F]-**3**. This material is available free of charge via the Internet at http://pubs.acs.org.

References

(1) Bräuner-Osborne, H.; Egebjerg, J.; Nielsen, E. O.; Madsen, U.; Krogsgaard-Larsen, P. Ligands for glutamate receptors: Design and therapeutic prospects. *J. Med. Chem.* **2000**, *43*, 2609−2645.

(2) Conn, P. J.; Pin, J. P. Pharmacology and functions of metabotropic glutamate receptors. *Ann. Rev. Pharmacol. Toxicol*. **1997**, *37*, 205−237.

(3) Pin, J.-P.; Acher, F. The metabotropic glutamate receptors: Structure, activation mechanism, and pharmacology. *Curr. Drug Targets: CNS Neurol. Disord.* **2002**, *1*, 297−317.

(4) Gasparini, F.; Lingenhohl, K.; Stoehr, N.; Flor, P. J.; Heinrich, M.; Vranesic, I.; Biollaz, M.; Allgeier, H.; Heckendorn, R.; Urwyler, S.; Varney, M. A.; Johnson, E. C.; Hess, S. D.; Rao, S. P.; Sacaan, A. I.; Santori, E. M.; Velicelebi, G.; Kuhn, R. 2-Methyl-6-(phenylethynyl)-pyridine (MPEP), a potent, selective and systemically active mGlu5 receptor antagonist. *Neuropharmacology* **1999**, *38*, 1493−1503.

(5) Cosford, N. D. P.; Roppe, J.; Tehrani, L.; Schweiger, E. J.; Seiders, T. J.; Chaudary, A.; Rao, S.; Varney, M. A. [^{3}H]-Methoxymethyl-MTEP and [^{3}H]-methoxy-PEPy: Potent and selective radioligands for the metabotropic glutamate subtype 5 (mGlu5) receptor. *Bioorg. Med. Chem. Lett.* **2003**, *13*, 351−354.

(6) Pietraszek, M.; Nagel, J.; Gravius, A.; Schäfer, D.; Danysz, W. The role of group I metabotropic glutamate receptors in schizophrenia. *Amino Acids* **2006**, *32*, 173−178.

(7) Tsai, V. W. W; Scott, H. L.; Lewis, R. J.; Dodd, P. R. The role of group I metabotropic glutamate receptors in neuronal excitotoxicity in Alzheimer's disease. *Neurotoxic. Res.* **2005**, *7*, 125−141.

(8) Brodkin, J.; Busse, C.; Sukoff, S. J.; Varney, M. A. Anxiolytic-like activity of the mGluR5 antagonist MPEP: A comparison with diazepam and buspirone. *Pharmacol., Biochem. Behav.* **2002**, *73*, 359−366.

(9) Cosford, N. D. P.; Tehrani, L.; Roppe, J.; Schweiger, E.; Smith, N. D.; Anderson, J. J.; Bristow, L.; Brodkin, J.; Jiang, X. H.; McDonald, I.; Rao, S.; Washburn, M.; Varney M. A. 3-[(2-Methyl-1,3-thiazol-4-yl)ethynyl]-pyridine: A potent and highly selective metabotropic glutamate subtype 5 receptor antagonist with anxiolytic activity *J. Med. Chem.* **2003**, *46*, 204−206.

(10) (a) Walker, K.; Reeve, A.; Bowes, M.; Winter, J.; Wotherspoon, G.; Davis, A.; Schmid, P.; Gasparini, F.; Kuhn, R.; Urban, L. mGlu5 receptors and nociceptive function II. mGlu5 receptors functionally expressed on peripheral sensory neurones mediate inflammatory hyperalgesia. *Neuropharmacology* **2001**, *40*, 10−19. (b) Walker, K.; Bowes, M.; Panesar, M.; Davis, A.; Gentry, C.; Kesingland, A.; Gasparini, F.; Spooren, W.; Stoehr, N.; Pagano, A.; Flor, P. J.; Vranesic, I.; Lingenhoehl, K.; Johnson, E. C.; Varney, M.; Urban, L.; Kuhn, R. Metabotropic glutamate receptor subtype 5 (mGlu5) and nociceptive function I. Selective blockade of mGlu5 receptors in models of acute, persistent and chronic pain. *Neuropharmacology* **2001**, *40*, 1−9.

(11) (a) Tessari, M.; Pilla, M.; Andreoli, M.; Hutcheson, D. M.; Heidbreder, C. A. Antagonism at metabotropic glutamate 5 receptors inhibits nicotine- and cocaine-taking behaviours and prevents nicotine-triggered relapse to nicotine-seeking. *Eur. J. Pharmacol.* **2004**, *499*, 121−133. (b) Chiamulera, C.; Epping-Jordan, M. P.; Zocchi, A.; Marcon, C.; Cottiny, C.; Tacconi, S.; Corsi, M.; Orzi, F.; Conquet, F. Reinforcing and locomotor stimulant effects of cocaine are absent in mGluR5 null mutant mice. *Nat. Neurosci.* **2001**, *4*, 873−874.

(12) Kenny, P. J.; Markou, A. The ups and downs of addiction: Role of metabotropic glutamate receptors. *Trends Pharmacol. Sci.* **2004**, *25*, 265−272.

(13) (a) Olive, F. M.; Mcgeehan, A. J.; Kinder, J. R.; McMahon, T.; Hodge, C. W.; Janak, P. H.; Messing, R. O. The mGluR5 antagonist 6-methyl-2-(phenylethynyl)pyridine decreases ethanol consumption via a protein kinase C-epsilon-dependent mechanism. *Mol. Pharmacol.* **2005**, *67*, 349−355. (b) Bäckström, P.; Bachteler, D.; Koch, S.; Hyytiä, P.; Spanagel, R. mGluR5 antagonist MPEP reduces ethanol-seeking and relapse behavior. *Neuropsychopharmacology* **2004**, *29*, 921−928.

(14) (a) Kokic, M.; Honer, M.; Ametamey, S. M.; Gasparini, F.; Andres, H.; Bischoff, S.; Flor, P. J.; Heinrich, M.; Vranesi, I; Spooren, W.; Kuhn, R.; Schubiger, P. A. Radiolabeling and in vivo evaluation of ^{11}C-M-MPEP as a PET radioligand for the imaging of the metabotropic glutamate receptor 5 (mGLuR5). *J. Labelled Compd. Radiopharm.* **2001**, *44* (Suppl. 1), S231−S232. (b) Musachio, J. L.; Ghose, S.; Toyama, H.; Kozikowski, A. P.; Klaess, T.; Mukhopadhyaya, J. K.; Ichise, M.; Hong, J.; Zoghbi, S.; Liow, J.-S.; Innis, R. B.; Pike, V. W. Two potential mGuR5 PET radioligands [^{11}C]M-MPEP and [^{11}C]methoxy-PEPy−Synthesis and initial PET evaluation in rats and monkeys. *Mol. Imaging Biol.* **2003**, *5*, 168.

(15) (a) Hamill, T. G.; Seiders, T. J.; Krause, S.; Ryan, C.; Sanabria, S.; Gibson, R. E.; Patel, S.; Cosford, N.; Roppe, J.; Yang, J.; King, C.; Hargreaves, R. J.; Burns, H. D. The synthesis and characterization of mGLuR5 receptor PET ligands. *J. Labelled Compd. Radiopharm.* **2003**, *46* (Suppl 1), S184. (b) Krause, S. M.; Hamill, T. G.; Seiders, T. J.; Ryan, C.; Sanabria, S.; Gibson, R. E.; Patel, S.; Cosford, N. D.; Roppe, J. R.; Hargreaves, R. J.; Burns, H. D. In vivo characterization of PET ligands for the mGluR5 receptor in rhesus monkey. *Mol. Imaging Biol*. **2003**, *5*, 166.

(16) Ametamey, S. M.; Kessler, L. J.; Honer, M.; Wyss, M. T.; Buck, A.; Hintermann, S.; Auberson, Y. P.; Gasparini, F.; Schubiger, P. A. Radiosynthesis and preclinical evaluation of ^{11}C-ABP688 as a probe for imaging the metabotropic glutamate receptor subtype 5. *J. Nucl. Med*. **2006**, *47*, 698−705.

(17) Ametamey, S. M.; Treyer, V.; Streffer, J.; Wyss, M. T.; Schmidt, M.; Blagoev, M.; Hintermann, S.; Auberson, Y.; Gasparini, F.; Fischer, U. C.; Buck, A. Human PET studies of metabotropic glutamate receptor subtype 5 with ^{11}C-ABP688. *J. Nucl. Med*. **2007**, *48*, 247−252.

(18) Hamill, T. G.; Krause, S.; Ryan, C.; Bonnefous, C.; Govek, S.; Seiders, T. J.; Cosford, N. D. P.; Roppe, J.; Kamenecka, T.; Patel, S.; Gibson, R. E.; Sanabria, S.; Riffel, K.; Eng, W.; King C.; Yang, X.; Green, M. D.; O'Malley, S. S.; Hargreaves, R.; Burns, H. D. Synthesis, characterization, and first successful monkey imaging studies of metabotropic glutamate receptor subtype 5 (mGluR5) PET radiotracers. *Synapse* **2005**, *56*, 205−216.

(19) Sonogashira, K.; Tohda, Y.; Hagihara, N. A convenient synthesis of acetylenes: Catalytic substitutions of acetylenic hydrogen with bromoalkenes, iodoarenes, and bromopyridines. *Tetrahedron Lett.* **1975**, *50*, 4467−4470.

(20) Dondoni, A.; Perrone, D. Total synthesis of (+)-galactostatin. An illustration of the utility of the thiazole-aldehyde synthesis. *J. Org. Chem*. **1995**, *60*, 4749− 4754.

(21) Nicolaou, K. C.; King, N. P.; Finlay, M. R. V.; He, Y.; Roschangar, F.; Vourloumis, D.; Vallberg, H.; Sarabia, F.; Ninkovic, S.; Hepworth, D. Total synthesis of epothilone E and related side-chain modified analogues via a Stille coupling based strategy. *Bioorg. Med. Chem.* **1999**, *7*, 665−697.

(22) Pike, V. W. Positron-emitting radioligands for studies in vivo—Probes for human psychopharmacology. *J. Psychopharmacol.* **1993**, *7*, 139−158.

(23) Waterhouse, R. N. Determination of lipophilicity and its use as a predictor of blood−brain barrier penetration of molecular imaging agents. *Mol. Imaging Biol.* **2003**, *5*, 376−389.

(24) Iso, Y.; Grajkowska, E.; Wroblewski, J. T.; Davis, J.; Goeders, N. E.; Johnson, K. M.; Sanker, S.; Roth, B. L.; Tueckmantel, W.; Kozikowski, A. P. Synthesis and structure−activity relationships of 3-[(2-methyl-1,3-thiazol-4-yl)ethynyl]pyridine analogues as potent, noncompetitive metabotropic glutamate receptor subtype 5 antagonists; search for cocaine medications. *J. Med. Chem.* **2006**, *49*, 1080−1100.

(25) Briard, E.; Pike V. W. Substitution−reduction: An alternative process for the [^{18}F]*N*-(2-fluoroethylation) of anilines. *J. Labelled Compd. Radiopharm.* **2004**, *47*, 217−232.

(26) See http://www.uppsala.imanet.se/research-synthia.asp for a description of similar apparatus.

(27) Patel, S.; Krause, S. M.; Hamil, T.; Chaudhary, A.; Burns, D. H.; Gibson, R. A. In vitro characterization of [^{3}H]methoxyPEPy, an mGluR5 selective radioligand. *Life Sci.* **2003**, *73*, 371−379.

(28) Scheibye, S.; Pedersen, B. S.; Lawesson, S.-O. Studies on organophosphorus compounds XXI. The dimer of *p*-methoxythionophosphine sulfide as a thiation reagent. A new route to thiocarboxamides. *Bull. Soc. Chim. Belg*. **1978**, *87*, 229−237.

(29) Zoghbi, S. S.; Baldwin, R. M.; Seibyl, J.; Charney, D. S.; Innis, R. B. A radiotracer technique for determining apparent pK_a of receptor binding ligands. *J. Labelled Compd. Radiopharm.* **1997**, *41*, 136−138.

(30) Lazarova, N.; Siméon, F. G.; Musachio, J. L.; Lu, S.; Pike, V. W. Integration of a microwave reactor with Synthia to provide a fully automated radiofluoridation module. *J. Labelled Compd. Radiopharm.* **2007**, *50*, 1−3.

(31) Clark, J. D.; Baldwin, R. L.; Bayne, K. A.; Brown, M. J.; Gebhart, G. F.; Gonder, J. C.; Gwathmey, J. K.; Keeling, M. E.; Kohn, D. F.; Robb, J. W.; Smith, O. A.; Steggerda, J.-A. D.; Van de Berg, J. L. *Guide for the Care and Use of Laboratory Animals*; National Academy Press: Washington DC, 1996.

(32) Carson, R. E.; Barker, W. C.; Liow, J.-S.; Johnson, C. A. *Conference Record of the IEEE Nuclear Science Symposium and Medical Imaging Conference*; Portland, Oregon, 2003.

JM0701268